***Research Article***

Chemical Review and Letters
journal homepage: www.chemrevlett.com
ISSN (online): 2645-4947 (print) 2676-7279

# DFT study on sensing possibility of the pristine and Al- and Ga-doped $B_{12}N_{12}$ nanostructures toward hydrazine and hydrogen peroxide and their analogues

Soma Majedi [a, *], Hwda Ghafur Rauf [a], Mohsen Boustanbakhsh[b]

[a] *College of Health Sciences, University of Human Development, Sulaimaniyah, Kurdistan region of Iraq*
[b] *Department of Chemistry, Payame Noor University, Tehran, Iran*

ARTICLE INFO

*Article history:*
Received 1 November 2019
Received in revised form 26 November 2019
Accepted 27 January 2020
Available online 14 February 2020

*Keywords:*
$N_2H_4$
$P_2H_4$
$O_2H_2$
$S_2H_2$
pristine
Al- and Ga-doped
$B_{12}N_{12}$ nanostructures, Density functional theory
DFT

ABSTRACT

We have perused the absorbency of $N_2H_4$, $P_2H_4$, $O_2H_2$ and $S_2H_2$ molecules on the exterior level of pristine and Al- and Ga-doped $B_{12}N_{12}$ nanostructures using through density functional theory (DFT) calculations. The consequences indicate that most favorable adsorption configurations are those in which the nitrogen atom of hydrazine ($N_2H_4$) is closed to boron, Aluminum and Gallium atoms of pristine and Al- and Ga-doped $B_{12}N_{12}$ nanostructures, respectively, with adsorption energies circa -1.801, -2.397, and -2.071 eV. Geometry optimizations, energy calculations and NBO charge transfer were used to evaluate the impression ability of $B_{12}N_{12}$ for various medium. The computed density of states (DOS) displays that a notable orbital hybridization be take place between $N_2H_4$ $P_2H_4$, $O_2H_2$ and $S_2H_2$ molecules with pristine and Al- and Ga-doped $B_{11}N_{12}$ nanostructures adsorption process. Finally, we concluded that the Al-doped $B_{11}N_{12}$ is more desirable than that of the pristine for $N_2H_4$ adsorption.

## 1. Introduction

Hydrazine ($N_2H_4$) is a colorless piteous liquid with an ammonia-like odor, and also is highly toxic and dangerously unstable unless used in solution. Toxic by aspiration and by skin absorption and corrosive to texture and Produces toxic oxides of nitrogen during combustion. As well as used as a rocket propellant and in fuel cells [1-6]. Hydrazine is a highly reactive base and reducing factor used in many industrial and medical applications. In biological applications, hydrazine and its formatives exhibit antidepressant virtues by inhibiting monoamine oxidase (MAO), an enzyme that catalyzes the deamination and inactivation of certain stimulatory neurotransmitters such as norepinephrine and dopamine [7,8]. Diphosphine ($P_2H_4$) is a no color liquid of several dual phosphorus hydrides. It is the contamination that typically causes samples of phosphine to take fire in air. Diphosphane accepts the dilettante conformation (like hydrazine, less symmetrical than shown in the image) with a P-P distance of 2.219 angstroms. It is nonbasic, unstable at room temperature, and spontaneously flammable in air. It is only poorly soluble in water but dissolves in organic solvents. Several experimental and theoretical studies have been carried out on $P_2H_4$ [9,10]. Hydrogen peroxide ($O_2H_2$) is a colorless liquid, slightly more viscous than water; however, for safety reasons it is normally used as a solution, and also it is a nonplanar molecule with (twisted) $C_2$ symmetry. Although the O−O bond is a single bond, the molecule has a relatively high rotational barrier of 2460 $cm^{-1}$ (29.45 kJ/mol) [11] The increased barrier is ascribed to repulsion between the lone pairs of the adjoining oxygen atoms and outcomes in hydrogen peroxide showing atropisomerism. Hydrogen disulfide is ($H_2S_2$) is a pale yellow volatile liquid with a camphor-like odor. The structure of hydrogen disulfide is similar to that of hydrogen peroxide, with $C_2$ point group symmetry. The two central sulfur atoms and two outer

∗ Corresponding author. e-mail: soma.majedi@uhd.edu.iq

hydrogen atoms are not coplanar. The H−S−S bond in hydrogen disulfide has a near-standard 90° torsion angle of the syn conformer. Molecular dimensions in these two molecules are: O−O, O−H, S−S and S−H bonds have lengths of 1.490, 0.970, 2.055 and 1.352 Å, respectively, [12, 13]. $B_{12}N_{12}$ nanostructures engrossed substantial regard due to their significant chemical and physical confidants, exclusively of extensive gap semiconductors [14–18]. Boron nitride nanostructures such as nanotubes [19], nanocapsules [20], and fullerenes have received much consideration as undertaking materials for the electronic industry because of their inimitable structures and confidants [21]. The $B_{12}N_{12}$ nanostructures energetically the most consistent cage between various types of $(BN)_n$ structures [22]. Fowler et al. [23] theoretically indicated that the $B_{12}N_{12}$ cage is the more stable between $B_{12}N_{12}$, $B_{16}N_{16,}$ $B_{28}N_{28}$ nanoclusters. In addition, theoretical studies displayed that the $B_{12}N_{12}$ cage created from foursquare and hexagonal rings, is more stable than one created from pentagons and hexagons [24–28]. Owing to the remarkable charge breakaway between the boron and nitrogen atoms, the boron atom (electron deficient) and nitrogen atom (electron rich) are Lewis acid and base, respectively. Therefore, $B_{12}N_{12}$ nanocluster can be considered as a nanometal catalyst with Lewis acid-base pairs. Ahmadi and co-workers [29] have indicated the theoretical outcomes of the $CO_2$ adsorption upon the $B_{12}N_{12}$ nanostructure, stating an exothermic and substantial process. Bahrami et al. have presented the betterment in the adsorption energy and electronic properties of amphetamine on the pristine, P- and Al-doped $B_{11}N_{12}$ nano-cages [30]. They have stated that the adsorption of amphetamine on the $AlB_{11}N_{12}$ is more eligible than that of the $PB_{11}N_{12}$ nano-cage. Shakerzadeh et al. theoretically showed phosgene adsorption behavior onto pristine, Al- and Ga-doped $B_{12}N_{12}$ and $B_{16}N_{16}$ nanoclusters [31]. Esrafili and co-workers [32] have offered the adsorption treatment of hydrazine ($N_2H_4$) on the surface of silicon-carbide nanotubes (SiCNTs) at CAM-B3LYP/6-31G* method of density functional theory. So, these considerable studies cheer us to survey the interaction of $N_2H_4$, $P_2H_4$, $O_2H_2$ and $S_2H_2$ Sensors on pristine and Al- and Ga-doped $B_{12}N_{12}$ nanostructures using density functional theory calculations.

## 2. Results and Discussion

### *2.1. Optimized the pristine and Al- and Ga-doped B12N12 nanostructures confidants*

Fig. 1 indicates the optimized structures of the pristine and Al- and Ga-doped $B_{12}N_{12}$ nanostructures at the M062X/aug-cc-pvdz//M062X/6-31+G* level. The B–N, Al–N and Ga–N bond length between two six-membered rings are about 1.483, 1.485 and 1.483 Å and that is between a foursquare and a six-membered ring is 1.439, 1.786 and 1.845 Å. The energy gap ($E_g$) of the pristine and Al- and Ga-doped B12N12 nanostructures are calculated to be about 9.050, 6.617 and 6.150 eV, offer a semiconducting identity. The highest occupied molecular orbital (HOMO) and the lowest un-occupied molecular orbital (LUMO) of the pristine and Al- and Ga-doped $B_{12}N_{12}$ nanostructures are localized on the N and Group 13 atoms, respectively, indicating that the Group 13 atoms of nano-cages functions as Lewis acid site and the nitrogen atom of nano-cages functions as Lewis base site.

### *2.2. Adsorption of $N_2H_4$ on the $B_{12}N_{12}$ and Al- and Ga-doped $B_{12}N_{12}$ nanostructures*

Four highly toxic and dangerously molecules, including $N_2H_4$, $P_2H_4$, $O_2H_2$ and $S_2H_2$, were chosen as target adsorbents. We perform structural optimization on the $B_{12}N_{12}$ and Al- and Ga-doped $B_{12}N_{12}$ nanostructures with and without each of $N_2H_4$, $P_2H_4$, $O_2H_2$ and $S_2H_2$ molecules to examine the energetic, equilibrium geometries and electronic confidants. More detailed information including values of $E_{ads}$, acceptor-donor interaction distance, Natural bonding orbital (NBO) analysis and the $\Delta E_g$ (change of $E_g$ of cage upon the adsorption process) are rostered in Table 1. In the next step we investigated the absorption of explained molecules one by one.

#### *2.2.1. Adsorption of $N_2H_4$ on the nanostructures*

Fig. 1 presentations optimized structures of the full the pristine and Al- and Ga-doped $B_{12}N_{12}$ nanostructures in interaction with $N_2H_4$ molecule at the M062X/aug-cc-pvdz//M062X/6-31+G* level of calculations. After the geometry optimization, stable configurations were observed for $N_2H_4$ from its N-side close to the B, Al and Ga atoms of the pristine and Al- and Ga-doped $B_{12}N_{12}$ nanostructures. The adsorption energies ($E_{ads}$) for adsorption of $N_2H_4$ molecule on the pristine and Al- and Ga-doped $B_{12}N_{12}$ nanostructures are circa -1.801, -2.397 and -2.071 eV, and acceptor-donor interaction distance are 1.605, 1.969 and 2.030 Å, respectively. The natural bond orbitals (NBO) charge analysis shows a net charge transfer of 0.352, 0.189 and 0.202 e from N of $N_2H_4$ to Group 13 atoms (B, Al and Ga) in the cage surface, showing high ionic nature of these bonds. Calculated MEP shows that the $N_2H_4$ molecule acts as an electron donor and the cages as an electron acceptor.

To describe this result, we carry out a FMO analysis on the $N_2H_4$ molecule, showing that its energy gaps for the pristine and Al- and Ga-doped $B_{12}N_{12}$ nanostructures are about 8.032, 7.232 and 7.033 eV imply to their semiconductor identities.

*2.2.2. Adsorption of $P_2H_4$ on the nanostructures*

Tree configurations have been weighed in order to study the adsorption of $P_2H_4$ on the pristine and Al- and Ga-doped $B_{12}N_{12}$ nanostructures. The Phosphorus head of $P_2H_4$ adsorbed on the top of B, Al and Ga atoms of the nanostructures (Fig. 1). The calculations show that the adsorption of $P_2H_4$ molecule on the top of B, Al and Ga atoms are exothermic processes with negative $E_{ads}$ of -0.541, -1.438 and -1.380 eV and acceptor-donor interaction distance of 2.052, 2.432 and 2.434 Å (Fig. 1). The mentioned interactions lead to charge transfer of 0.609, 0.323 and 0.352 e from the $P_2H_4$ to the pristine and Al- and Ga-doped $B_{12}N_{12}$ nanostructures (Table 1), informing that the $P_2H_4$ acts as an electron donor and the cages as an electron acceptor. The calculated MEP (Fig. 2) obviously displays where the red color on the adsorbed $P_2H_4$ demonstrates the negative charge. The FMO analysis on the $P_2H_4$ molecule, showing that the interactions between the Phosphorus of $P_2H_4$ and B, Al and Ga atoms of the pristine and Al- and Ga-doped $B_{12}N_{12}$ nanostructures, hence HOMO on the P atom and LUMO on the B, Al and Ga of the nanostructures, respectively, (Fig. 3).

*2.2.3. Adsorption of $O_2H_2$ on the nanostructures*

The optimized structures of $O_2H_2$ on the pristine and Al- and Ga-doped $B_{12}N_{12}$ nanostructures are presented in Fig. 1. For $B_{12}N_{12}$-$O_2H_2$, $AlB_{11}N_{12}$-$O_2H_2$ and $GaB_{11}N_{12}$-$O_2H_2$ complexes adsorption energy and acceptor-donor interaction distance are -0.821, -1.635 and -1.399 eV and 1.654, 1.899 and 2.023 Å, respectively, attend with a charge transfer of 0.247, 0.107 and 0.116 e from $O_2H_2$ to the nanostructures (Table 1). We displayed electrostatic potentials at the 0.001 electrons per $Bohr^{-3}$ isodensity surfaces of $O_2H_2$ adsorption on the nanostructures were calculated with WFA surface analysis suite in fig 2 [36]. The $O_2H_2$ molecule can transfer the electrons to the LUMO on the boron, aluminum and gallium site of the cages through the electron lone pair of oxygen atom of $O_2H_2$ and HOMO on the B site of the (Fig. 3). The $E_g$ for $B_{12}N_{12}$-$O_2H_2$, $AlB_{11}N_{12}$-$O_2H_2$ and $GaB_{11}N_{12}$-$O_2H_2$ complexes are 8.435, 7.194 and 7.255 eV, respectively (Table 1).

*2.2.4. Adsorption of $S_2H_2$ on the nanostructures*

We studied the adsorption of $S_2H_2$ on the pristine and Al- and Ga-doped $B_{12}N_{12}$ nanostructures. The optimized structures of monomers and complexes are shown in Fig. 1. The calculated adsorption energies ($E_{ad}$) and acceptor-donor interaction distance for complexes are -0.377 eV and 2.150 Å ($B_{12}N_{12}$-$S_2H_2$), -1.236 eV and 2.412 Å ($AlB_{11}N_{12}$-$S_2H_2$) and -1.133 eV and 2.452 Å ($GaB_{11}N_{12}$-$S_2H_2$). The NBO calculations reveal that the charge transfers for $B_{12}N_{12}$-$S_2H_2$, $AlB_{11}N_{12}$-$S_2H_2$ and $GaB_{11}N_{12}$-$S_2H_2$ complexes are 0.432, 0.276 and 0.289 e from $S_2H_2$ molecule to the $B_{12}N_{12}$, $AlB_{11}N_{12}$ and $GaB_{11}N_{12}$ nanostructures surfaces, respectively, (Table 1). Therefore, the boron, aluminum and gallium atoms functions as Lewis acid site and the sulfur atom molecule functions as Lewis base site. The electrostatic potential map of $B_{12}N_{12}$-$S_2H_2$, $AlB_{11}N_{12}$-$S_2H_2$ and $GaB_{11}N_{12}$-$S_2H_2$ complexes that represents the positions of the several most positive and most negative potentials, defined as $V_{S,max}$ and $V_{S,min}$, respectively in Fig 2. The HOMO, LUMO energies and affiliated band gaps of $B_{12}N_{12}$-$S_2H_2$, $AlB_{11}N_{12}$-$S_2H_2$ and $GaB_{11}N_{12}$-$S_2H_2$ systems (Table 1). HOMO–LUMO gap ($E_g$) for mention systems are about 7.486, 6.102 and 6.049 eV, respectively, demonstrating that the nanostructures are a semi-insulator combination (Fig 3).

A comparatively major difference of adsorption energy in the $X_2H_4$-$M_{12}N_{12}$ and $Y_2H_2$-$M_{12}N_{12}$ (X=N, P, Y=O, S and M=B, Al, Ga) complexes can be said on the basis of electronegativity difference, p character, and dipole moment in molecules (see Table 2). Attraction established between the cationic (electropositive part) B, Al and Ga of $B_{12}N_{12}$, $AlB_{11}N_{12}$ and $GaB_{11}N_{12}$ and anion (electronegative part) N, P, O and S of $N_2H_4$, $P_2H_4$, $O_2H_2$ and $S_2H_2$ molecules.

*2.3. Density of state (DOS) analysis*

To investigate the adsorption effects of the $N_2H_4$, $P_2H_4$, $O_2H_2$ and $S_2H_2$ molecules on the electronic virtues of $B_{12}N_{12}$, $AlB_{11}N_{12}$ and $GaB_{11}N_{12}$ nanostructures, density of state (DOS) maps for the most stable states of the nanostructures have been shown in Fig. 4. Computed DOS display the $E_g$ of BN, Al-doped $B_{12}N_{12}$ and Ga-doped $B_{12}N_{12}$ is 9.050, 6.617 and 6.150 eV, and also the energy gaps (and the change of HOMO–LUMO gap) of $B_{12}N_{12}$-$N_2H_4$, $B_{12}N_{12}$-$P_2H_4$, $B_{12}N_{12}$-$O_2H_2$, $AlB_{11}N_{12}$-$N_2H_4$, $AlB_{11}N_{12}$-$P_2H_4$, $AlB_{11}N_{12}$-$P_2H_4$, $AlB_{11}N_{12}$-$S_2H_2$, $AlB_{11}N_{12}$-$N_2H_4$, $AlB_{11}N_{12}$-$P_2H_4$, $AlB_{11}N_{12}$-$P_2H_4$ and $AlB_{11}N_{12}$-$S_2H_2$ nanostructures are 8.032 (101.827%), 7.965 (108.576%), 8.435 (61.499%), 7.486 (156.415%), 7.232 (61.445%), 6.907

(28.981%), 7.194 (57.662%), 6.102 (51.567%), 7.033 (88.249%), 6.724 (57.363%), 7.255 (110.454%) and

6.049 (10.096%) eV, respectively, at the M062X/aug-cc-pvdz//M062X/6-31+G* level (Fig. 4)

The computed DOS shows that the $E_g$ value is reduced compared to the isolated BN, Al-doped $B_{12}N_{12}$ and Ga-doped $B_{12}N_{12}$. It is recognized that the $E_g$ is a main factor in designation of the electrical conductivity of BN, Al-doped $B_{12}N_{12}$ and Ga-doped $B_{12}N_{12}$ which will improve in the existence of the molecules with respect to the following equation [37]:

$$\sigma \propto \exp\left(\frac{-E_g}{2KT}\right)$$

in where σ is the electrical conductivity and k is the Boltzmann's constant. According to the equation, the smaller $E_g$ value leads to increase the conductivity at a given temperature. However, it can be conclude that the BN, Al-doped $B_{12}N_{12}$ and Ga-doped $B_{12}N_{12}$ nanostructures selectively functions as a gas sensor system between $N_2H_4$, $P_2H_4$, $O_2H_2$ and $S_2H_2$ which functions as the most suitable gas sensor for the $N_2H_4$ molecule.

## 3. Experimental

Geometry optimizations, energy calculations, density of states (DOS) [33] analysis, adsorption energy, natural bond orbital (NBO) [34] analysis, highest occupied molecular orbital (HOMO), lowest unoccupied molecular orbital (LUMO) and band gap have been carried out using M062X functional with 6-31+G* basis set as accomplished in GAMESS suite of program [35] GaussSum program [33] was application to obtain DOS results. Vibrational frequencies have been calculated at the identical level to corroborate that all of the static points correspond to true minima (no imaginary frequency) on the potential energy surface (PES) [36].

The adsorption energy ($E_{ad}$) of the molecule on the $B_{12}N_{12}$ and $AlB_{11}N_{12}$ nanoclusters surface is defined as follows:

$$E_{ad} = E_{\text{Molecule/nanoparticle}} - \left(E_{\text{nanoparticle}} + \text{E}_{\text{Molecule}}\right)$$

**Table 1**. Calculated acceptor-donor interaction distance ($d_{\text{Molecule/ nanostructures}}$), adsorption energy ($E_{ad}$: eV), HOMO energies ($E_{HOMO}$), LUMO energies ($E_{LUMO}$) and HOMO–LUMO energy gap ($E_g$) for mentioned systems.

| complexes | $d_{Acceptor...Donor}$ | $E_{ad}$ | $Q_{NBO}$ | $E_{HOMO}$ (eV) | $E_{LUMO}$ (eV) | $E_g$ (eV) | [a]$\Delta E_g$ (%) (eV) |
|---|---|---|---|---|---|---|---|
| $B_{12}N_{12}$ | — | — | — | -9.440 | -0.389 | 9.050 | — |
| $B_{12}N_{12}$-$N_2H_4$ | 1.605 | -1.801 | 0.352 | -8.757 | -0.725 | 8.032 | 101.827 |
| $B_{12}N_{12}$-$P_2H_4$ | 2.052 | -0.541 | 0.609 | -8.684 | -0.719 | 7.965 | 108.576 |
| $B_{12}N_{12}$-$O_2H_2$ | 1.654 | -0.821 | 0.247 | -9.048 | -0.613 | 8.435 | 61.499 |
| $B_{12}N_{12}$-$S_2H_2$ | 2.150 | -0.377 | 0.432 | -8.881 | -1.395 | 7.486 | 156.415 |
| $AlB_{11}N_{12}$ | — | — | — | -9.006 | -2.389 | 6.617 | — |
| $AlB_{11}N_{12}$-$N_2H_4$ | 1.969 | -2.397 | 0.189 | -8.425 | -1.193 | 7.232 | 61.445 |
| $AlB_{11}N_{12}$-$P_2H_4$ | 2.432 | -1.438 | 0.323 | -8.352 | -1.445 | 6.907 | 28.981 |
| $AlB_{11}N_{12}$-$O_2H_2$ | 1.899 | -1.635 | 0.107 | -8.652 | -1.458 | 7.194 | 57.662 |
| $AlB_{11}N_{12}$-$S_2H_2$ | 2.412 | -1.236 | 0.276 | -8.417 | -2.316 | 6.102 | 51.567 |
| $GaB_{11}N_{12}$ | — | — | — | -8.975 | -2.825 | 6.150 | — |
| $GaB_{11}N_{12}$-$N_2H_4$ | 2.030 | -2.071 | 0.202 | -8.293 | -1.260 | 7.033 | 88.249 |
| $GaB_{11}N_{12}$-$P_2H_4$ | 2.434 | -1.380 | 0.352 | -8.221 | -1.497 | 6.724 | 57.363 |
| $GaB_{11}N_{12}$-$O_2H_2$ | 2.023 | -1.399 | 0.116 | -8.680 | -1.425 | 7.255 | 110.454 |
| $GaB_{11}N_{12}$-$S_2H_2$ | 2.452 | -1.133 | 0.289 | -8.331 | -2.281 | 6.049 | 10.096 |

[a]The change of HOMO–LUMO gap of $B_{12}N_{12}$, $AlB_{11}N_{12}$ and $GaB_{11}N_{12}$ after adsorption. All energies are in eV. All distances are in Å. $Q_{NBO}$ is in e.

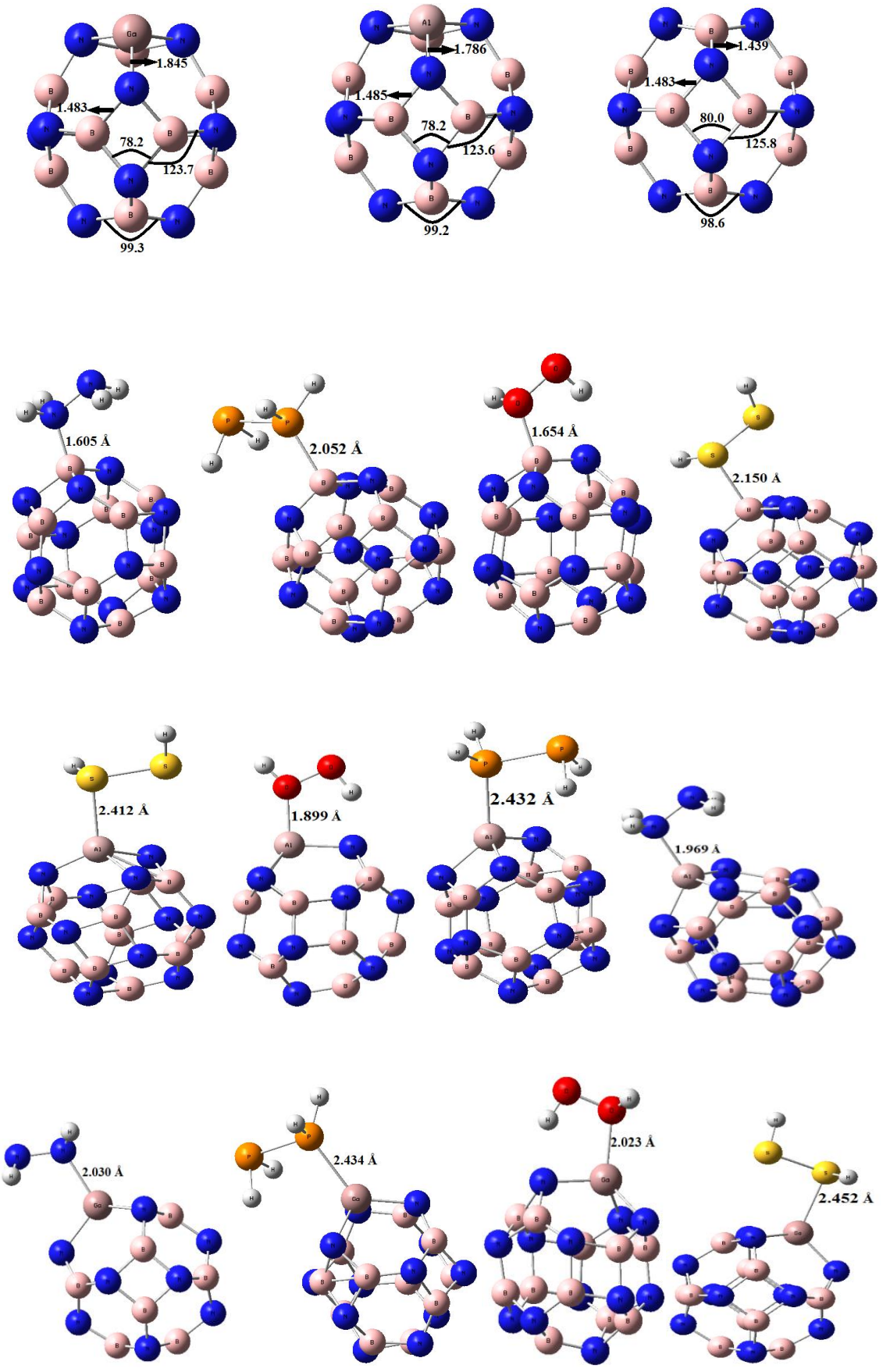


**Fig. 1.** Geometric parameters of pure $B_{12}N_{12}$, $AlB_{11}N_{12}$, $GaB_{11}N_{12}$ monomers, $X_2H_4$-$M_{12}N_{12}$ and $Y_2H_2$-$M_{12}N_{12}$ (X=N, P, Y=O, S and M=B, Al, Ga) complexes. Distances in Å and angles in degrees.

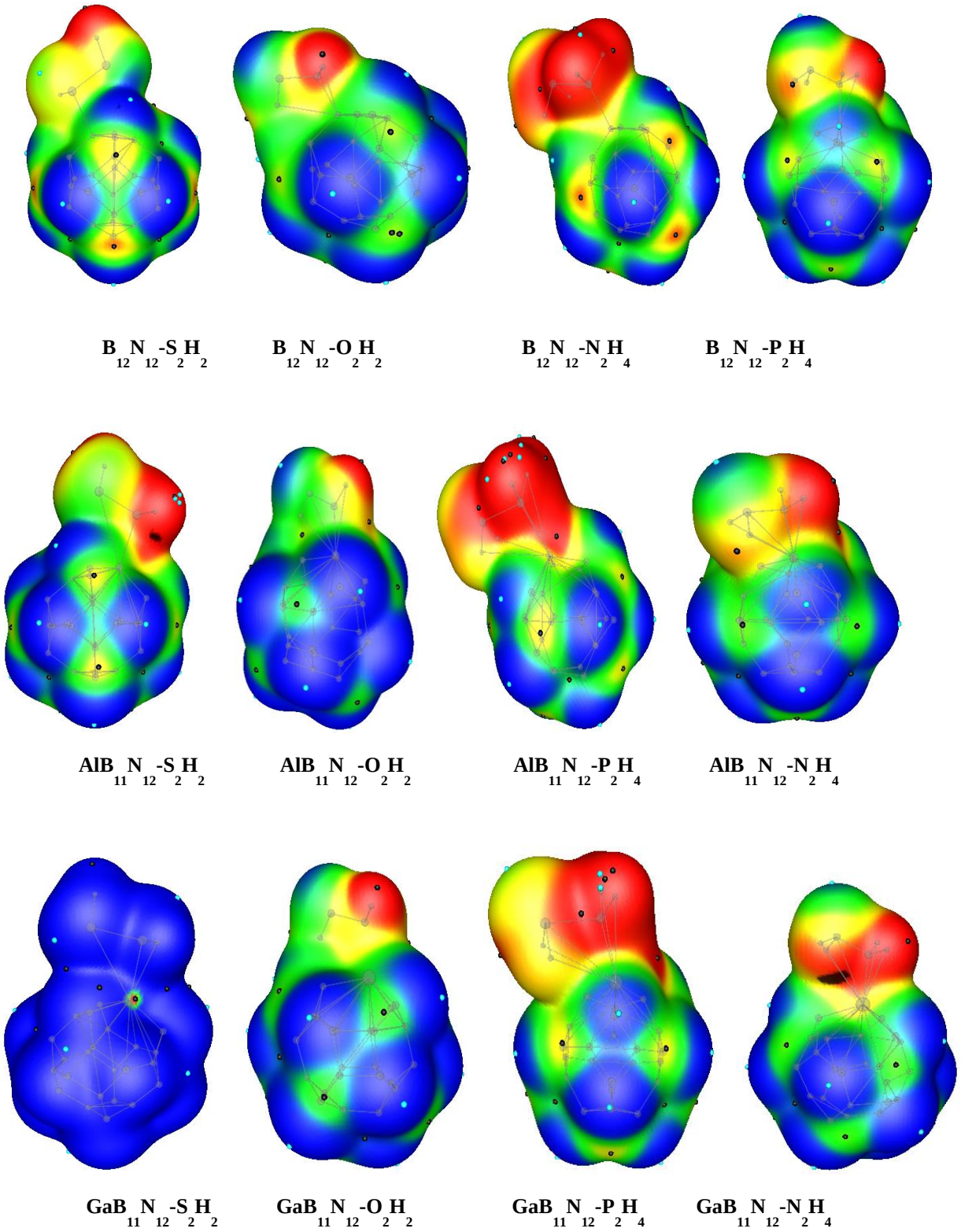


**Fig 2.** Electron density difference (EDD) maps isosurfaces ( ± 0.001 au) of pure and complexes

where, $E_{\text{Molecule/nanoparticle}}$, $E_{\text{Molecule}}$ and $E_{\text{nanoparticle}}$ are the total energy of Molecule─ nanoparticle system in the equation state, the energy of a single Molecule, and the energy of the free nanostructures, respectively. All $E_{ad}$ values were obtained using M062X/aug-cc-pvdz//M062X/6-31+G* level.

| NAME | HOMO | LUMO |
|---|---|---|
| $B_{12}N_{12}$ | 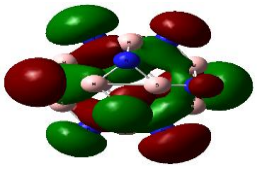 | 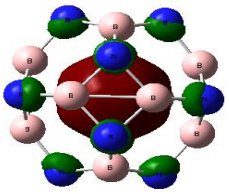 |
| $AlB_{11}N_{12}$ | 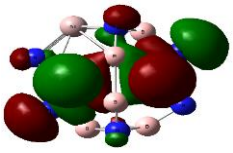 | 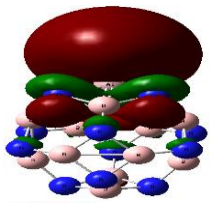 |
| $GaB_{11}N_{12}$ | 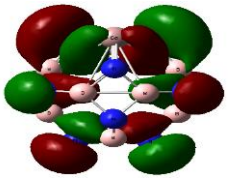 | 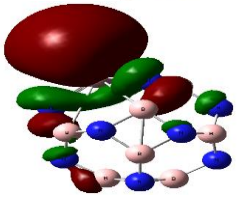 |
| $N_2H_4$ | 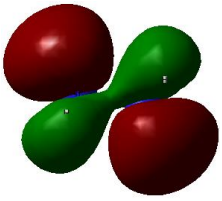 | 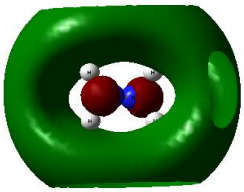 |
| $P_2H_4$ | 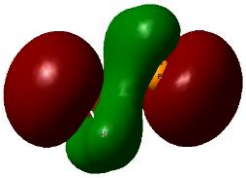 | 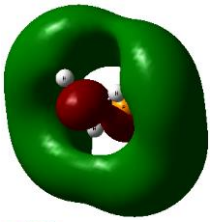 |
| $O_2H_2$ | 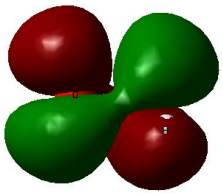 | 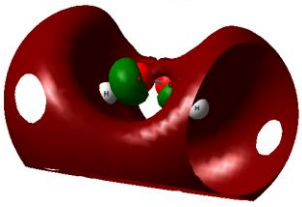 |
| $S_2H_2$ | 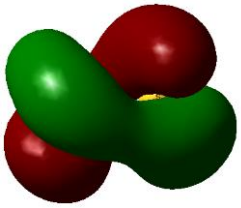 | 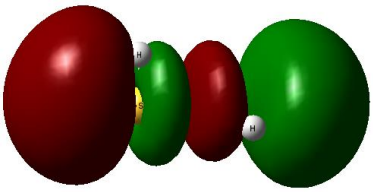 |
| $B_{12}N_{12}$-$N_2H_4$ | 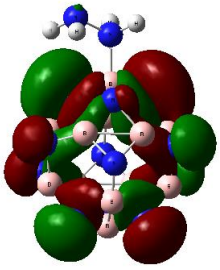 | 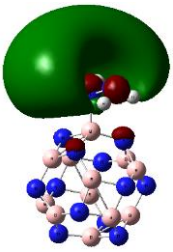 |

| NAME | HOMO | LUMO |
|---|---|---|
| $B_{12}N_{12}-P_2H_4$ | 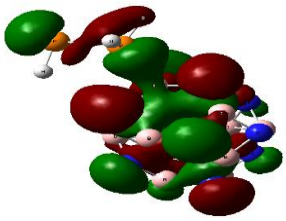 | 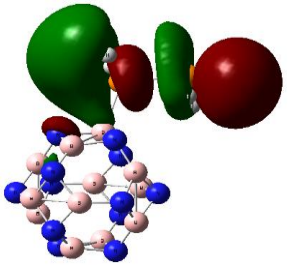 |
| $B_{12}N_{12}-O_2H_2$ | 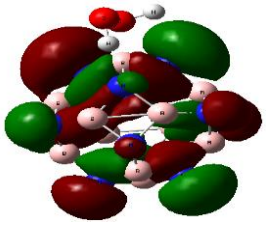 | 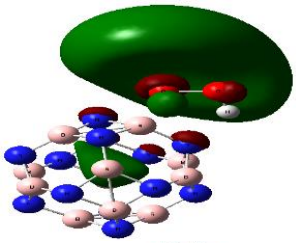 |
| $B_{12}N_{12}-S_2H_2$ | 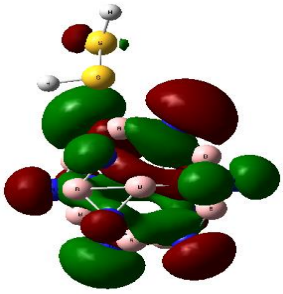 | 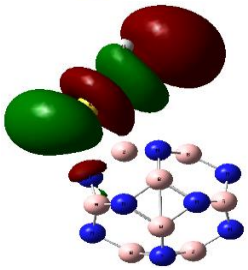 |
| $AlB_{11}N_{12}-N_2H_4$ | 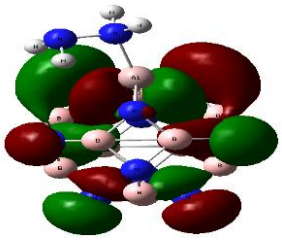 | 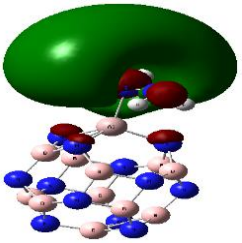 |
| $AlB_{11}N_{12}-P_2H_4$ | 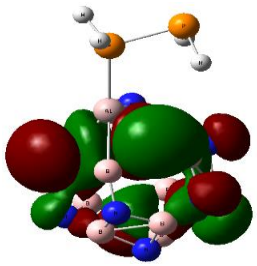 | 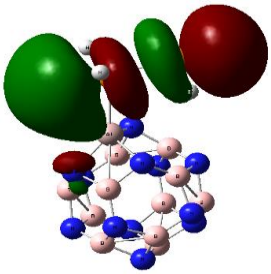 |
| $AlB_{11}N_{12}-O_2H_2$ | 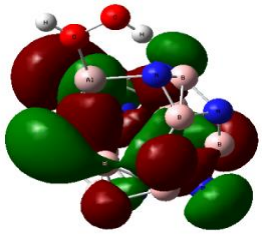 | 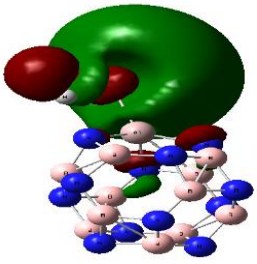 |

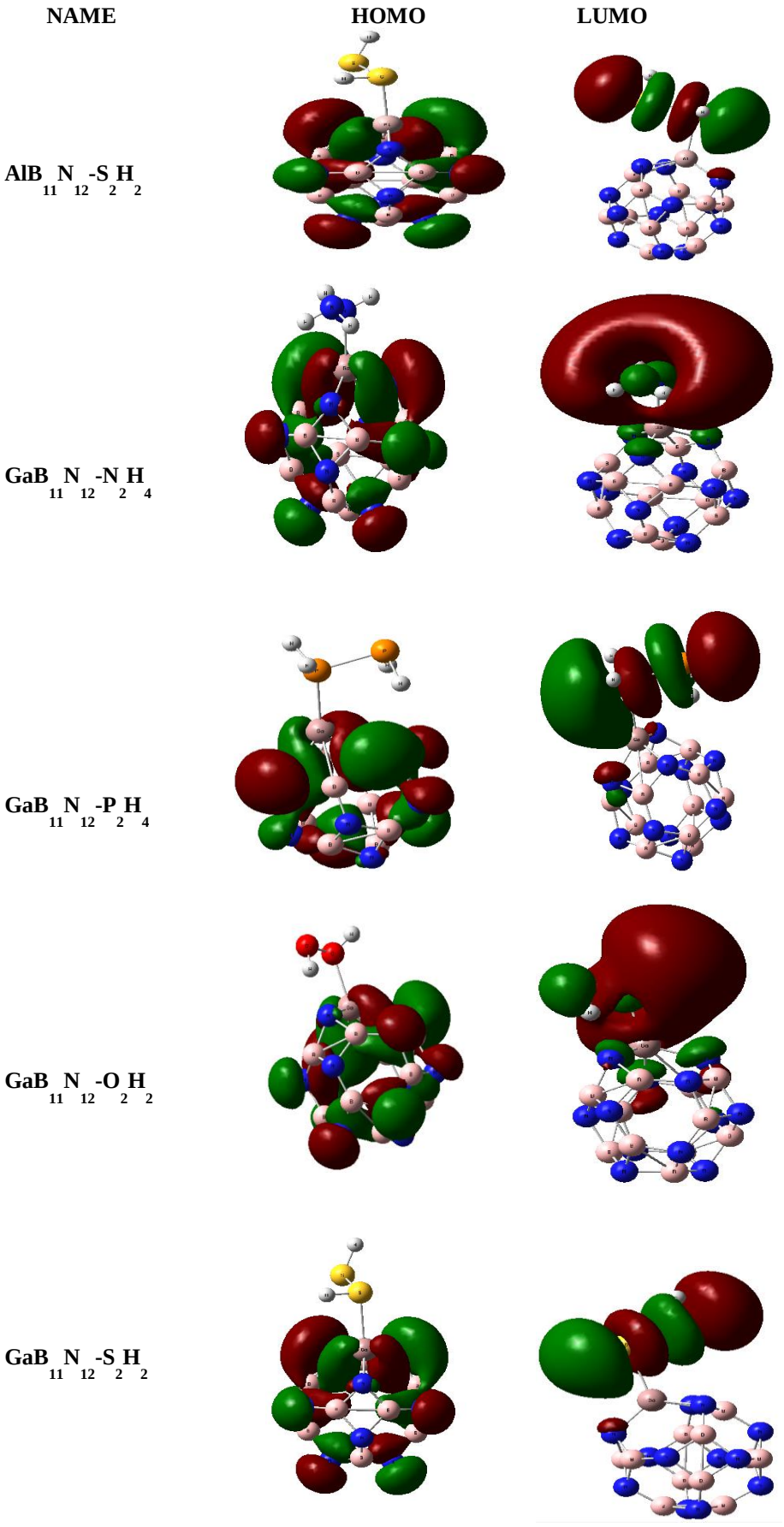


**Fig. 3** Frontier orbitals of mentioned Configurations

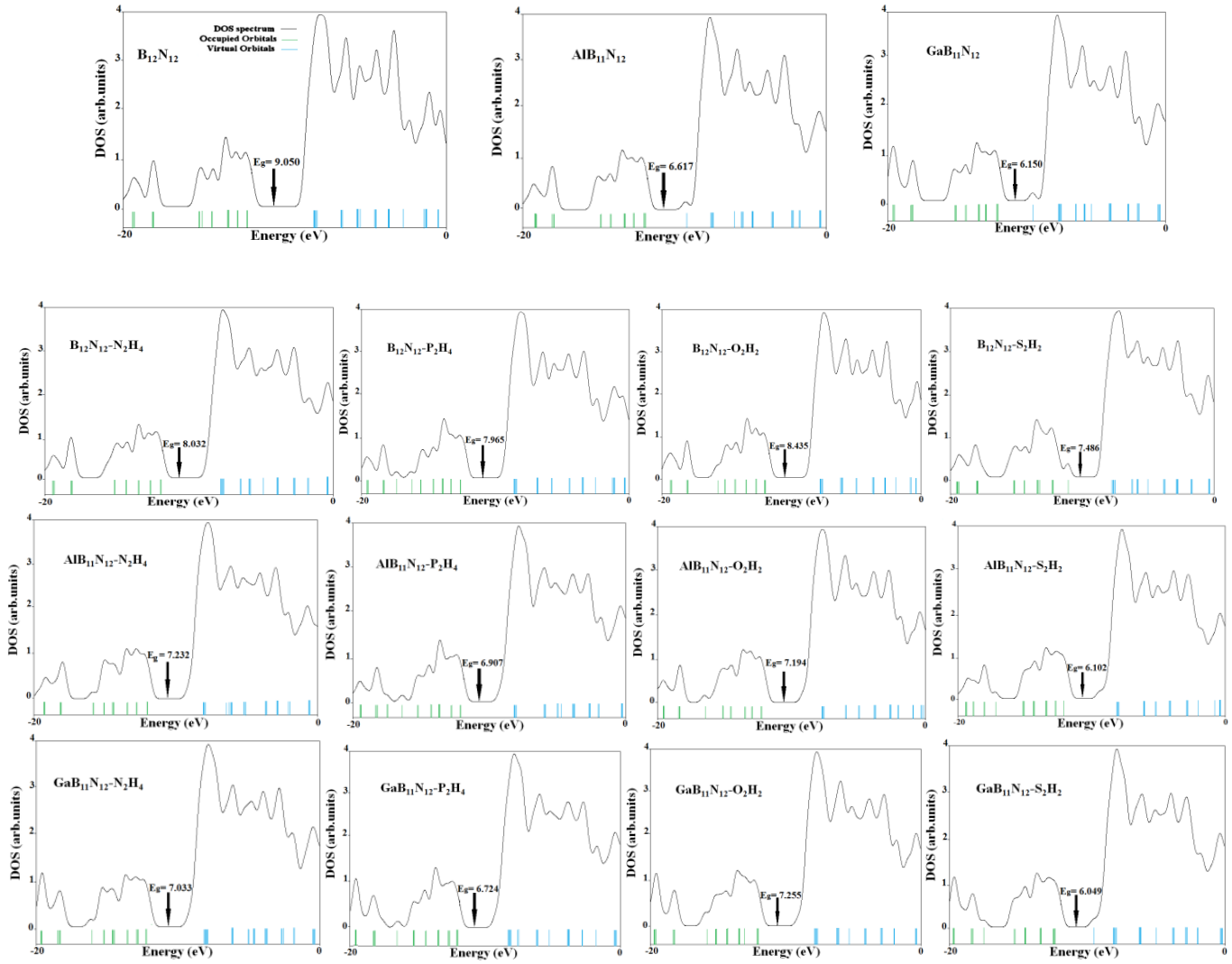


**Fig. 4.** Computed density of states (DOS) for pure BNN, $AlB_{11}N_{12}$, $GaB_{11}N_{12}$ monomers, $X_2H_4$-$M_{12}N_{12}$ and $Y_2H_2$-$M_{12}N_{12}$ (X=N, P, Y=O, S and M=B, Al, Ga) complexes.

**Table 2.** HOMO energies ($E_{HOMO}$), LUMO energies ($E_{LUMO}$) and HOMO–LUMO energy gap ($E_g$), dipole moment (D) and electronegativity of $X_2H_4$ and $Y_2H_2$ (X=N, P and Y=O, S)

| monomer | $E_{HOMO}$ (eV) | $E_{LUMO}$ (eV) | $E_g$ (eV) | dipole moment (D) | electronegativity |
|---|---|---|---|---|---|
| $N_2H_4$ | -7.490 | -0.122 | 7.367 | 0.052 | 3.806 |
| $P_2H_4$ | -7.831 | -0.210 | 7.622 | 0.001 | 4.020 |
| $O_2H_2$ | -9.982 | -0.209 | 9.774 | 1.689 | 5.096 |
| $S_2H_2$ | -8.726 | -0.549 | 8.177 | 1.197 | 4.637 |

## 4. Conclusions

DFT calculations were carry out to study adsorption of $X_2H_4$ and $Y_2H_2$ (X=N, P and Y=O, S) molecules on the outer surface of BN, Al-doped $B_{12}N_{12}$ and Ga-doped $B_{12}N_{12}$ nanostructures. The M062X/aug-cc-pvdz//M062X/6-31+G* level calculations are used to studied the equilibrium distances, stabilities, and electronic properties of $N_2H_4$, $P_2H_4$, $O_2H_2$ and $S_2H_2$ molecules which adsorbed at top of the BN, Al-doped $B_{12}N_{12}$ and Ga-doped $B_{12}N_{12}$ nanostructures. The results reveal that the most stable configuration is $AlB_{11}N_{12}$-$N_2H_4$ nanostructure with adsorption energy ($E_{ads}$) circa -2.397 eV and 61.445% the change of HOMO–LUMO gap ($\Delta E_g$ (%)). A comparatively major difference of adsorption energy in the $X_2H_4$-$M_{12}N_{12}$ and $Y_2H_2$-$M_{12}N_{12}$ (X=N, P, Y=O, S and M=B, Al, Ga) complexes can be said on the basis of electronegativity difference, p character, and dipole moment in molecules. Eventually, we believe that the present study can be helpful for designing and developing $N_2H_4$ based on BN, Al-doped $B_{12}N_{12}$ and Ga-doped $B_{12}N_{12}$

nanostructures, and also it is concluded that BN, Al-doped $B_{12}N_{12}$ and Ga-doped $B_{12}N_{12}$ nanostructure has excellent reflex selectivity toward $N_2H_4$ compared to $P_2H_4$, $O_2H_2$ and $S_2H_2$ molecules.

**References**


[1] Centers for Disease Control. Retrieved 16 August (2012).

[2] The PubChem Project. USA: National Center for Biotechnology Information. March 13-17, 2016

[3] National Institute for Occupational Safety and Health (NIOSH). December 29, 1970; 45 years ago

[4] H. K. Hall, Correlation of the Base Strengths of Amines. *J. Am. Chem. Soc.*, 79 (1957) 5441-5444.

[5] A. Earnshaw, Chemistry of the Elements (2nd ed.). Butterworth-Heinemann, ISBN 0-08-037941-9 (1997).

[6] B. Martel and K. Cassidy, Chemical Risk Analysis: A Practical Handbook. Butterworth–Heinemann. (2004) p. 361. ISBN 1-903996-65-1.

[7] Immediately Dangerous to Life and Health. National Institute for Occupational Safety and Health (NIOSH).

[8] J.-P. Schirmann and P. Bourdauducq, Wiley-VCH, Weinheim, (2002) doi:10.1002/14356007.a13_177.

[9] D. Chakraborty, P. Chandra, Ab initio molecular orbital calculations of nuclear spin–spin coupling constants in PH−2, PH3, PH+4 and P2H4. *J. Mol. Struc.*, 434 (1998) 75-84.

[10] V. Galasso, Green's function ab initio study of the outer valence ionization energies of N2H4, P2H4, As2H4, PH2NH2, PF2NH2 and AsH2NH2. *J. Elec. Spec. Rel. Phen.*, 32 (1983) 359-369.

[11] D. W. Davies, Photoelectron spectra of hydrogen peroxide and hydrogen disulphide: ab initio calculations. *Chem. Phys. Lett.*, 28 (1974) 520–522.

[12] P. Lazzeretti and R. Zanasi, On the calculation of parity-violating energies in hydrogen peroxide and hydrogen disulphide molecules within the random-phase approximation. *Chem. Phys. Lett.*, 279 (1997) 349–354.

[13] H. Hunt, Robert, Leacock, A. Robert, C. Peters Wilbur, T. Hecht Karl., Internal-Rotation in Hydrogen Peroxide: The Far-Infrared Spectrum and the Determination of the Hindering Potential. J. Chem. Phys. 42 (1965) 1931.

[14] R. T. Paine, C. K. Narula, Synthetic routes to boron nitride. *Chem. Rev.*, 90 (1990) 73-91.

[15] H. S. Wu, F. Q. Zhang, X. H. Xu, C. J. Zhang, H. Jiao, Geometric and Energetic Aspects of Aluminum Nitride Cages. *J. Phys. Chem. A.*, 107 (2003) 204-209.

[16] H.Y. Zhu, T.G. Schmalz, D.J. Klein, Alternant boron nitride cages: A theoretical study. *Int. J. Quantum Chem.*, 63 (1997) 393-401.

[17] D. Goldberg, Y. Bando, O. Stepahan, K. Kurashima, Octahedral boron nitride fullerenes formed by electron beam irradiation. *Appl. Phys. Lett.*, 73 (1998) 2441.

[18] Q. Wang, Q. Sun, P. Jena, Y. Kawazoe, Potential of AlN Nanostructures as Hydrogen Storage Materials. *ACS Nano.*, 3 (2009) 621-626.

[19] N.G.Chopra, R. J. Luyken, K. Cherrey, V. H. Crespi, M.L. Cohen, S.G. Louie, A. Zettl, Boron Nitride Nanotubes. *Science.*, 269 (1995) 966-967.

[20] I. Narita, T. Oku, Effects of catalytic metals for synthesis of BN fullerene nanomaterials. *Diamond. Relat. Mater.*, 12 (2003) 1146-1150.

[21] S. Iijima, C. J. Brabec, A.Maiti, J. Bernholc, Structural flexibility of carbon nanotubes. *J. Chem. Phys.*, 104 (1996) 2089-2092.

[22] S. Xu, M. Zhang, Y. Zhao, B. Chen, J. Zhang, C.C. Sun, Stability and property of planar (BN)x clusters. *Chem. Phys. Lett.*, 423 (2006) 212-214.

[23] G. Seifert, R. Fowler, D. Mitchell, D. Porezag, T. Frauenheim, Boron-nitrogen analogues of the fullerenes: electronic and structural properties. *Chem. Phys. Lett.*, 268 (1997) 352-358.

[24] D. Strout, Structure and Stability of Boron Nitrides: Isomers of B12N12. *J. Phys. Chem. A.*, 104 (2000) 3364-3366.

[25] D. Strout, L. Strout. Structure and Stability of Boron Nitrides: The Crossover between Rings and Cages. *J. Phys. Chem. A.*, 105 (2001) 261-263.

[26] F. Jensen, H. Toftlund, Structure and stability of C24 and B12N12 isomers. *Chem. Phys. Lett.*, 201 (1993) 89-96.

[27] T. Oku, A. Nishiwaki and I. Narita, Formation and atomic structure of B12N12 nanocage clusters studied by mass spectrometry and cluster calculation. *Sci. Technol. Adv. Mater.*, 5 (2004) 635-638.

[28] T. Oku, M. Kuno, H. Kitahara, I. Nartia, Formation, atomic structures and properties of boron nitride and carbon nanocage fullerene materials. *Int. J. Inorg. Mater.*, 3 (2001) 597-612.

[29] M. T. Baei, A. Ahmadi Peyghan, Z. Bagheri, A DFT Study on CO2 Interaction with a BN Nano-Cage. *Bull. Korean Chem. Soc.*, 33 (2012) 3338–3342.

[30] A. Bahrami, S. Seidi, T. Baheri, M. Aghamohammadi, A first-principles study on the adsorption behavior of amphetamine on pristine, P- and Al-doped B12N12 nano-cages. *Superlattic. Microstruct.*, 64 (2013) 265–273.

[31] E. Shakerzadeh, E. Khodayar, S. Noorizadeh, Theoretical assessment of phosgene adsorption behavior onto pristine, Al- and Ga-doped B12N12 and B16N16 nanoclusters. *Comput. Mater. Sci.*, 118 (2016) 155–171.

[32] M. D. Esrafili, V. Mokhtar Teymurian, R. Nurazar, Catalytic dehydrogenation of hydrazine on silicon-carbide nanotubes: A DFT study on the kinetic issue. *Surf. Sci.*, 632 (2015) 118–125.

[33] N. O'Boyle, A. Tenderholt and K. Langner, cclib: A library for package independent computational chemistry algorithms. *J. Comput. Chem.*, 29 (2008) 839–845.

[34] F. Weinhold and C.R. Landis, Discovering Chemistry With Natural Bond Orbitals, John Wiley & Sons, (2012).

[35] M. W. Schmidt, K. K.Baldridge, J. A.Boatz, S. T. Elbert, M. S. Gordon, J. H. Jensen, S. Koseki, N. Matsunaga, K. A. Nguyen and S. Su, General atomic and molecular electronic structure system. *J. Comput. Chem.*, 14 (1993) 1347-1363

[36] F. A. Bulat, A. Toro-Labbe, T. Brinck, J. S. Murray, P. Politzer, Quantitative analysis of molecular surfaces: areas, volumes, electrostatic potentials and average local ionization energies. *J. Mol. Model.*, 16 (2010) 1679–1691.

[37] S.S. Li, Semiconductor physical electronics, 2nd edn. Springer, Heidelberg (2006)



## How to Cite This Article

Soma Majedi; Hwda Ghafur Rauf; Mohsen Boustanbakhsh. "DFT study on sensing possibility of the pristine and Al- and Ga-embeded B12N12 nanostructures toward hydrazine and hydrogen peroxide and their analogues". Chemical Review and Letters, 2, 4, 2019, 176-186. doi: 10.22034/crl.2020.216625.1032